Sensors and Actuators B 240 (2017) 487–496

Contents lists available at ScienceDirect

Sensors and Actuators B: Chemical

journal homepage: www.elsevier.com/locate/snb

An original ferroferric oxide and gold nanoparticles-modified glassy carbon electrode for the determination of bisphenol A

Edson R. Santana, Camila A. de Lima, Jamille V. Piovesan, Almir Spinelli*

Grupo de Estudos de Processos Eletroquímicos e Eletroanalíticos, Universidade Federal de Santa Catarina, Campus Universitário Reitor João David Ferreira Lima, Departamento de Química – CFM, 88040-900 – Florianópolis, SC, Brazil

ARTICLE INFO

Article history:
Received 8 June 2016
Received in revised form 22 July 2016
Accepted 2 September 2016
Available online 4 September 2016

Keywords:
Ferroferric oxide nanoparticles
Gold nanoparticles
Modified electrode
Bisphenol A
Voltammetry

ABSTRACT

A novel glassy carbon electrode (GCE) modified with a film of ferroferric oxide nanoparticles (Fe_3O_4 NPs) over a film of gold nanoparticles (Au NPs), both stabilized in a polymer solution of 3-*n*-propyl-4-picolinium silsesquioxane chloride ($Si4Pic^+Cl^-$), is presented for the electroanalytical determination of bisphenol A (BPA). At the modified electrode, cyclic voltammograms of BPA in B-R buffer (pH 9.0) showed a diffusion-controlled irreversible oxidation peak at around +0.470 V. Under optimized experimental conditions for differential pulse voltammetry experiments, the peak current was found to vary linearly with the concentration of BPA in the range of 20–1400 nmol L^{-1} ($R^2 = 0.996$) with a detection limit of 7.0 nmol L^{-1}. The modified electrode Fe_3O_4 NPs-$Si4Pic^+Cl^-$/Au NPs-$Si4Pic^+Cl^-$/GCE was successfully employed for the determination of BPA in different commercial plastic samples. Satisfactory recoveries were obtained in the range of 90–120%, in agreement with the comparative technique (UV–vis spectroscopy).

1. Introduction

Bisphenol A (BPA) is a compound widely used as a monomer in the synthesis of polycarbonate (PC) and epoxy resins, and along with other materials it is used to produce plastics. It is thus present in a wide variety of products including packaging for food and drinks, packing materials and engineering plastics, and it has been detected in samples of wastewater and drinking water [1–3]. However, BPA is non-biodegradable, highly resistant to chemical degradation and it has been listed as a typical endocrine disruptor, which can mimic hormones and may lead to negative health effects [4,5]. Small amounts of BPA may cause reproductive disorders including decreased sperm quality, birth defects and impaired brain development in humans, besides various kinds of cancer, such as prostate, testicular and breast cancer [6,7]. Considering these characteristics, analytical methods employing sensitive detectors need to be developed for the determination of BPA.

Several techniques are used to determine the BPA content in different matrices, which include high-performance liquid chromatography (HPLC) [8,9] and more sophisticated techniques such as liquid chromatography–tandem mass spectrometry (LC–MS-MS) [10] and gas chromatography coupled with mass spectrometry (GC–MS) [11]. However, it is well-known that separation methods involve expensive instrumentation, requiring time-consuming extraction or pre-concentration steps and skilled operators [3,12]. Furthermore, studies involving the use of fluorescence [13,14], the enzyme-linked immunosorbent assay (ELISA) [2,15], chemiluminescence [16,17] and electrochemical techniques [1,3–7] have been reported. Notable among these are the voltammetric techniques, which offer a number of advantages in environmental monitoring, such as fast response, low cost, ease of miniaturization, simple operation, accuracy, high sensitivity, good selectivity and *in vivo* real-time determination [3,4,18]. Although BPA is an electrochemically-active compound, the direct determination of BPA with bare electrodes is not applicable due to the poor response of the traditional unmodified electrodes to BPA. To solve this problem, novel sensing materials with high conductivity and stability as well as good catalytic activity need to be developed [4,19]. To improve the sensitivity and selectivity in the determination of BPA, various materials have been proposed for the modification of electrodes including ionic liquids [18,20], enzymes [21,22], molecularly imprinted polymers [23,24], many carbon materials, such as carbon nanotubes [25], both single-walled (SWCNT) [4] and multiple-walled (MWCNT)

* Corresponding author at: Universidade Federal de Santa Catarina – UFSC, Campus Universitário Reitor João David Ferreira Lima, Centro de Ciências Físicas e Matemáticas – CFM, Departamento de Química, 88040-900 – Florianópolis – SC – Brazil.
E-mail address: almir.spinelli@ufsc.br (A. Spinelli).

http://dx.doi.org/10.1016/j.snb.2016.09.003
0925-4005/

[26–28] and graphene [29–31] and metal nanoparticle-based composites, such as gold nanoparticles (Au NPs) [32,33] and ferroferric oxide nanoparticles (Fe_3O_4 NPs) [3,19,34,35].

Au NPs are widely used to build electrochemical devices due to their high chemical stability, excellent catalytic ability, good biocompatibility, high electrical conductivity and enhanced surface area, facilitating the electron transfer [32,36,37]. Many authors have reported that electrodes modified with Au NPs have shown excellent electrocatalytic activity for the detection of biomolecules [37–43]. Recently, Saha et al. [36] published a review on the synthesis and application of Au NPs in the fields of chemical and biological sensing. For the determination of BPA in milk samples, Zhou et al. [33] developed an aptasensor based on a glassy carbon electrode modified with an Au NPs-dotted graphene nanocomposite film. Also, Niu et al. [32] used a glassy carbon electrode modified with a stacked graphene nanofibers/Au NPs composite to determine the BPA content in a plastic baby bottle.

The unique characteristics of Fe_3O_4 NPs allow their application in many fields, as supports for the immobilization of biomaterials, in environmental treatment, in biomedical and bioengineering, and in food analysis [44]. Recently, Fe_3O_4 magnetic NPs have attracted increasing interest for application in sensing devices because, in addition to their small size and large surface area, their properties include strong superparamagnetism, biocompatibility, low toxicity, easy preparation and high adsorption ability [3,34]. As an example, Yu et al. [3] reported the application of a glassy carbon electrode modified with a chitosan-Fe_3O_4 nanocomposite for the amperometric determination of BPA in real plastic samples. Similarly, Zhang et al. [35] determined BPA in commercial plastic samples using a sensor based on Fe_3O_4 NPs-reduced graphene oxide composites stabilized in chitosan. The detection limit obtained was 17 nmol L^{-1}.

To retard the tendency toward the aggregation of metallic NPs they need to be dispersed in a suitable matrix which promotes enhanced stability. In this regard, organic-inorganic hybrid materials, such as silsesquioxanes, have been the subject of increasing interest since they offer a combination of the physical properties of glass, such as rigidity and thermal stability and the exchange properties of the organofunctional group. In addition, due to the presence of the ionic organic groups, these materials exhibit notable solubility in water. Recently some authors have reported that soluble charged silsesquioxanes, such as the water-soluble 3-*n*-propyl-4-picolinium silsesquioxane chloride (Si4Pic$^+$Cl$^-$), represent an excellent alternative to support and stabilize metal nanoparticles in aqueous medium besides having the ability to form stable thin films on various surfaces [43,45,46].

In this context, we propose a novel, simple, fast and sensitive electrochemical detector for BPA determination based on the good current response resulting from BPA oxidation at a glassy carbon electrode modified with a film of Fe_3O_4 NPs over a film of Au NPs, both NPs being stabilized by a Si4Pic$^+$Cl$^-$ polymer. The proposed chemically-modified electrode was employed to determine BPA in plastic samples. The precision and accuracy provided by the electrochemical detector were verified by recovery experiments and comparison with data provided by the UV–vis technique.

2. Experimental

2.1. Chemicals, reagents and solutions

All chemicals were of analytical grade and used without further purification. The aqueous solutions were prepared with water purified using a Milli-Q system (Millipore, United States) with a resistivity of 18.2 MΩ cm. Britton-Robinson (B-R) (H_3BO_3/CH_3COOH/H_3PO_4), Mcllvaine (citric acid/Na_2PO_4), NH_3/NH_4Cl, and H_3BO_3·KCl/NaOH buffers were prepared at an initial concentration of 0.1 mol L^{-1} and tested as the supporting electrolyte. The pH was adjusted with 1.0 mol L^{-1} HCl or NaOH solution. A stock solution of 0.1 mol L^{-1} $K_3[Fe(CN)_6]$ and a solution of 0.1 mol L^{-1} KCl were prepared in water. A stock solution of 1.0 mmol L^{-1} BPA in ethanol was prepared daily. The water-soluble 3-*n*-propyl-4-picolinium silsesquioxane chloride (Si4Pic$^+$Cl$^-$) polymer was kindly provided by the Laboratório de Equílibrios Químicos e Superfícies (LabEqS-UFSC). The synthesis and characterization of this material are described in the Ref. [43].

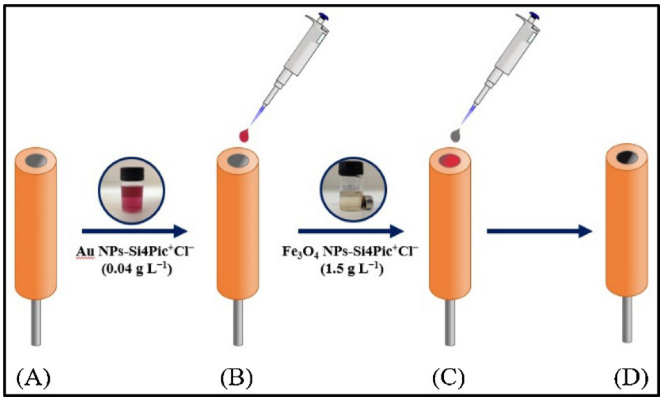

Scheme 1. Construction steps of the proposed modified electrode.

2.2. Preparation of the Au NPs-Si4Pic$^+$Cl$^-$ dispersion

Au NPs stabilized in the silsesquioxane polymer were prepared as follows: 5 μL of 0.1 mol L^{-1} chloroauric acid were added to 2.5 mL of an aqueous solution of Si4Pic$^+$Cl$^-$ (2.0 g L^{-1}). The mixture was stirred for 5 min at room temperature and 200 μL of a freshly prepared 20.0 m mol L^{-1} sodium borohydride solution were quickly added under continuous stirring. After 60 s the dispersion changed from colorless to red, indicating the formation of Au NPs. The dispersion obtained was stored at 4 °C.

2.3. Preparation of the Fe_3O_4 NPs-Si4Pic$^+$Cl$^-$ dispersion

The Fe_3O_4 magnetic nanoparticles of around 30 nm used in this study were purchased from Sigma-Aldrich. The nanoparticle dispersion was prepared by adding 3.75 mg of Fe_3O_4 NPs to 2.5 mL of an aqueous solution of Si4Pic$^+$Cl$^-$ (2.0 g L^{-1}). The mixture was stirred for 5 min at room temperature and stored at 4 °C.

2.4. Preparation of the modified electrode

As shown in Scheme 1, the drop coating method was used to prepare the as modified electrode as follows: (A) a bare GCE (diameter of 2 mm) was carefully polished with 0.05 μm alumina powder, thoroughly rinsed and sonicated for 3 min in purified ethanol; (B) an aliquot (3.0 μL) of the Au NPs-Si4Pic$^+$Cl$^-$ dispersion was then dropped onto the surface of the GCE and allowed to dry in a stove at 40 °C for 10 min; after drying, (C) an aliquot (3.0 μL) of the Fe_3O_4 NPs-Si4Pic$^+$Cl$^-$ dispersion was dropped onto the surface of the Au NPs-Si4Pic$^+$Cl$^-$-modified GCE and dried in a stove for 10 min; the as prepared (D) Fe_3O_4 NPs-Si4Pic$^+$Cl$^-$/Au NPs-Si4Pic$^+$Cl$^-$-modified GCE electrode.

2.5. Apparatus

To characterize the Au NPs-Si4Pic$^+$Cl$^-$ dispersion and perform the comparative method of analysis by UV–vis spectroscopy, a

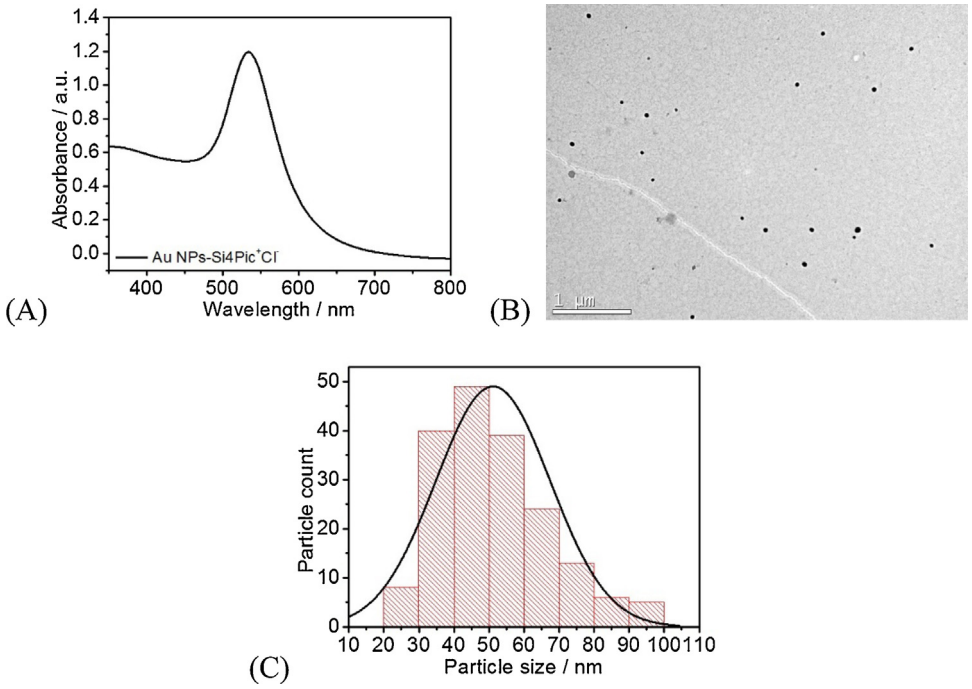

Fig. 1. (A) UV–vis spectrum, (B) TEM image and (C) particle size distribution for Au NPs-Si4Pic$^+$Cl$^-$.

UV-1800 spectrophotometer (Shimadzu, Japan) was employed. Images of the Au NPs-Si4Pic$^+$Cl$^-$ and Fe_3O_4 NPs-Si4Pic$^+$Cl$^-$ were obtained by transmission electron microscopy (TEM) using a JEM-2100 microscope (JEOL, Japan) operating at 100 kV. To obtain the TEM images of the Au NPs-Si4Pic$^+$Cl$^-$, a drop of the dispersion was placed on a carbon-coated copper grid and then dried at room temperature for 24 h. The same procedure was adopted for Fe_3O_4 NPs-Si4Pic$^+$Cl$^-$, but the drop was obtained from an aliquot of the supernatant of the dispersion. The nanoparticle diameter distribution was obtained using the ImageJ software. The morphology of the Fe_3O_4 NPs-Si4Pic$^+$Cl$^-$/Au NPs-Si4Pic$^+$Cl$^-$ immobilized on the glassy carbon surface was analyzed by scanning electron microscopy with field emission gun (SEM-FEG) using a JSM-6701F microscope (JEOL, Japan) (accelerating voltage of 10 kV). The images were obtained at the Central Laboratory for Electron Microscopy, UFSC. Electrochemical impedance spectroscopy (EIS) measurements were carried out using an Autolab PGSTAT128N potentiostat/galvanostat (Eco Chemie, The Netherlands) with an FRA impedance module using the open circuit mode, an amplitude of 5 mV and a frequency range of 0.1–100 000 Hz. The electrochemical experiments were carried out on a PalmSens portable potentiostat (Palms Instruments BV, The Netherlands) coupled to a personal computer with the PSTrace 4.6 software installed. A standard one-compartment three-electrode glass cell was used. A bare GCE or modified GCE served as the working electrode, a platinum wire as the auxiliary electrode and an Ag/AgCl (KCl saturated) as the reference electrode.

2.6. Sample preparation

In order to evaluate the performance of the modified electrode developed for practical analytical applications, the determination of BPA in commercial samples such as a polycarbonate (PC) cup, polystyrene (PS) plastic cup, polyvinyl chloride (PVC) food packaging, polyethylene terephthalate (PET) water bottle and BPA-free plastic containers was carried out via addition and recovery studies. All of the commercial samples were acquired from shops in Florianópolis, Santa Catarina State, Brazil. The treatment of the commercial samples used was based on the work published by Li et al. [26]. The commercial samples were pre-cleaned in an ultrasonic bath with acetone (with the exception of the PS sample, which was immersed in ethanol), rinsed successively with ethanol and ultrapure water and then dried. In the next step, the commercial samples were cut into small pieces and 1.0 g samples of these pieces together with 30 mL of ultrapure water were heated in an oil bath at 70 °C for 48 h. After cooling to room temperature and filtering, the resulting water-leached sample was collected. Lastly, ultrapure water was added to make up 100 mL. For the voltammetric analysis, an aliquot of 4.0 mL of water-leached sample was transferred to the electrochemical cell along with 6.0 mL of the supporting electrolyte. The standard addition method was used to evaluate the analytical performance of the modified electrode.

2.7. Comparative spectroscopic method

UV–vis spectroscopy was carried out in the wavelength range of 200–450 nm. A quartz cell with an optical path length of 1.0 cm was used. The absorbance of the solutions containing different concentrations of BPA was determined at 279 nm.

3. Results and discussion

3.1. Characterization of Au NPs-Si4Pic$^+$Cl$^-$ and Fe_3O_4 NPs-Si4Pic$^+$Cl$^-$ dispersions

The characterization of the Au NPs-Si4Pic$^+$Cl$^-$ was performed by TEM analysis and UV–vis spectroscopy. Fig. 1A shows the surface plasmon resonance absorption peak at 533 nm, which corresponds to an average particle diameter of around 50 nm [47,48]. These results are consistent with those obtained in the TEM analysis. Fig. 1B shows the TEM image of Au NPs-Si4Pic$^+$Cl$^-$ and Fig. 1C a histogram of the particle size distribution. The latter was constructed by counting approximately 200 particles randomly chosen from more than one TEM image. The TEM image shows that synthesized Au NPs were spherical in shape with an average size of 50 nm.

The characterization of the Fe_3O_4 NPs-Si4Pic$^+$Cl$^-$ was also carried out by TEM analysis. Fig. 2A shows the TEM image of Fe_3O_4

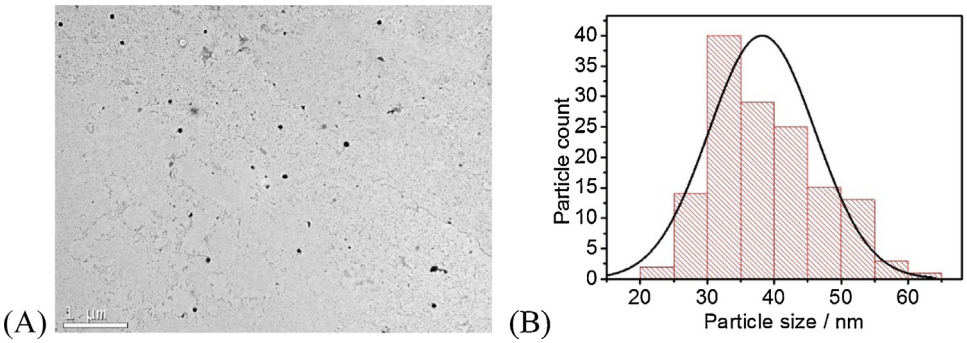

Fig. 2. (A) TEM image and (B) particle size distribution for Fe_3O_4 NPs-Si4Pic$^+$Cl$^-$.

NPs-Si4Pic$^+$Cl$^-$ and Fig. 2B the histogram with the particle size distribution constructed by counting approximately 200 particles randomly chosen from more than one TEM image. The average size of the Fe_3O_4 NPs dispersed in the polymer was 38 nm, which is close to the size certified by the manufacturer (30 nm).

3.2. Characterization of Fe_3O_4 NPs-Si4Pic$^+$Cl$^-$/Au NPs-Si4Pic$^+$Cl$^-$/GCE

The morphology of the GCE and Fe_3O_4 NPs-Si4Pic$^+$Cl$^-$/Au NPs-Si4Pic$^+$Cl$^-$/GCE was investigated by SEM-FEG. A clear difference in terms of surface morphology is observed between the bare GCE (Fig. 3A) and the GCE modified with Au NPs and Fe_3O_4 NPs (Fig. 3B). The presence of nanoparticles well distributed on the GCE substrate is evident. However, it is not possible to determine the chemical nature of the nanoparticles from the image.

Electrochemical impedance spectroscopy (EIS) was employed to characterize the interfacial properties of the modified electrode. The results are shown in Fig. 4 in the form of Nyquist diagrams. In EIS, the semicircle diameter of impedance equals the electron transfer resistance (R_{ct}), which controls the electron transfer kinetics of the redox probe at the electrode surface [6]. Fig. 4a shows the impedances of the bare GCE in 5.0 mmol L^{-1} $[Fe(CN)_6]^{3-/4-}$ containing 0.1 mol L^{-1} KCl. It can be seen that a large well-defined semicircle was obtained at lower frequencies, corresponding to R_{ct} = 757 ohm, indicating strong resistance to charge transfer. When Fe_3O_4 NPs-Si4Pic$^+$Cl$^-$ (Fig. 4b) or Au NPs-Si4Pic$^+$Cl$^-$ (Fig. 4c) dispersions were deposited on the surface of the GCE, the impedance values obtained decreased to R_{ct} = 586 ohm and R_{ct} = 606 ohm, respectively, which could be attributed to the conductivity of the Au NPs and Fe_3O_4 NPs, leading to a lower interface electrical resistance. Finally, when the two nanoparticle dispersions were dropped onto the surface of the GCE, the impedance value obtained at Fe_3O_4 NPs-Si4Pic$^+$Cl$^-$/Au NPs-Si4Pic$^+$Cl$^-$/GCE (Fig. 4d) was even lower, reaching R_{ct} = 158 ohm, indicating a lower charge transfer resistance. These experiments demonstrated the successful preparation of the chemically-modified GCE with Fe_3O_4 NPs over Au NPs.

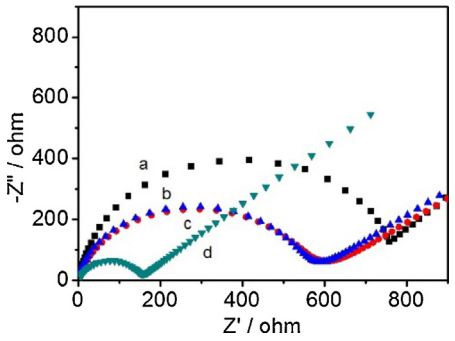

Fig. 4. Nyquist plots of different electrodes in 0.1 mol L^{-1} KCl containing 5.0 mmol L^{-1} $Fe(CN)_6^{3-/4-}$ solution: (a) GCE, (b) Fe_3O_4 NPs-Si4Pic$^+$Cl$^-$/GCE, (c) Au NPs-Si4Pic$^+$Cl$^-$/GCE, and (d) Fe_3O_4 NPs-Si4Pic$^+$Cl$^-$/Au NPs-Si4Pic$^+$Cl$^-$/GCE.

3.3. Electrochemical behavior of BPA at Fe_3O_4 NPs-Si4Pic$^+$Cl$^-$/Au NPs-Si4Pic$^+$Cl$^-$/GCE

As shown in Fig. 5, the electrochemical response of the different electrodes to BPA was investigated using cyclic voltammetry. When 10.0 μmol L^{-1} BPA was added to the pH 9.0 B-R buffer, a single oxidation peak was seen for all electrodes tested in the potential window from +0.2 to +1.2 V. This indicates that the oxidation reaction of BPA is an irreversible process, which is in agreement with previous reports [1,3,4,34]. This oxidation reaction took place on the bare GCE surface (curve a) at +0.500 V with an anodic current of 1.02 μA. For the modified electrodes, the oxidation peak and current were, respectively, +0.500 V and 1.12 μA for the Si4Pic$^+$Cl$^-$/GCE (curve b), +0.495 V and 2.45 μA for the Au NPs-Si4Pic$^+$Cl$^-$/GCE (curve c), +0.495 V and 3.12 μA for the Fe_3O_4 NPs-Si4Pic$^+$Cl$^-$/GCE (curve d) and +0.470 V and 4.47 μA for the

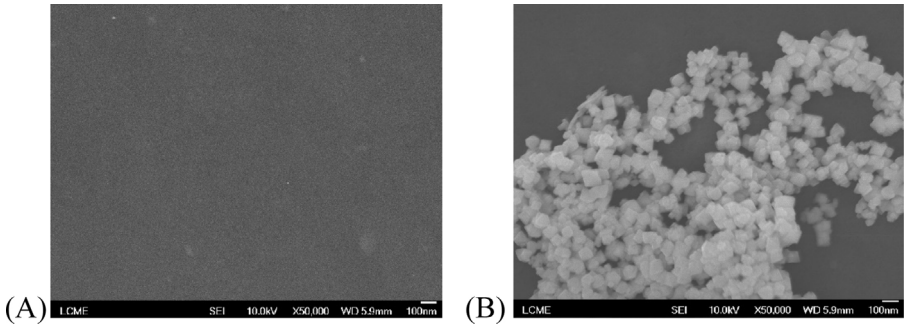

Fig. 3. SEM-FEG images for (A) GCE and (B) Fe_3O_4 NPs-Si4Pic$^+$Cl$^-$/Au NPs-Si4Pic$^+$Cl$^-$/GCE.

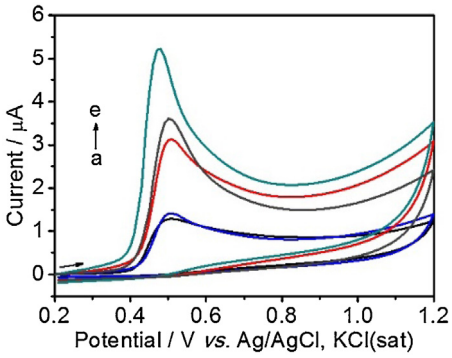

Fig. 5. Cyclic voltammograms obtained for different electrodes in B-R buffer (pH 9.0) containing 10.0 μmol L^{-1} BPA: (a) GCE, (b) Si4Pic$^+$Cl$^-$/GCE, (c) Au NPs-Si4Pic$^+$Cl$^-$/GCE (d) Fe_3O_4 NPs-Si4Pic$^+$Cl$^-$/GCE, and (e) Fe_3O_4 NPs-Si4Pic$^+$Cl$^-$/Au NPs-Si4Pic$^+$Cl$^-$/GCE electrodes, ν = 100 mV s^{-1}.

Fe_3O_4 NPs-Si4Pic$^+$Cl$^-$/Au NPs-Si4Pic$^+$Cl$^-$/GCE (curve e). Hence, the current for the BPA oxidation was four times higher for the Fe_3O_4 NPs/Au NPs modified electrode compared to the unmodified bare GCE. The increase in the anodic current is associated with the higher surface area of the modified electrode and good conductivity provided by the Fe_3O_4 NPs and Au NPs. Furthermore, regarding the peak potentials, for the modified electrodes the oxidation peak shifted 30 mV compared to the bare electrode, favoring the oxidation reaction. This result demonstrates the synergistic effect of Fe_3O_4 NPs and Au NPs, also increasing the catalytic activity of the modified electrode, verifying that it is suitable for the determination of BPA.

However, it was observed that for BPA the anodic currents decreased significantly with the cycle number. This occurred because the oxidation of BPA formed a polymeric product which blocked the electrode surface, as previously observed in other studies [1,3,27,37,49]. Therefore, measurements of the first cycle were used for the BPA analysis in the following studies.

The electrochemical behavior of BPA at the Fe_3O_4 NPs-Si4Pic$^+$Cl$^-$/Au NPs-Si4Pic$^+$Cl$^-$/GCE with different scan rates was studied further. The corresponding voltammograms are shown in Fig. 6A, where it can be seen that the oxidation peak currents increase linearly with the scan rate in the range of 10–300 mV s^{-1}. From these data, the plot of the logarithm of the peak current (log i) versus the logarithm of the scan rate (log ν) (Fig. 6B) was linear (R^2 = 0.975), with the equation of the straight line being log i = 0.534 log ν–0.999. According to the literature [50], a log–log plot slope of (or close to) 0.5 indicates a diffusion-controlled reaction rate. Therefore, we can conclude that the BPA oxidation reaction on Fe_3O_4 NPs-Si4Pic$^+$Cl$^-$/Au NPs-Si4Pic$^+$Cl$^-$/GCE is a diffusion-controlled process, corroborating with other studies reported in the literature [34,37].

In addition, the relationship between the anodic peak potential (E_{pa}) and the logarithm of the scan rate is shown in Fig. 6C. It can be seen that E_{pa} shifted linearly with log ν (R^2 = 0.986), with a linear regression equation of E_{pa} = 0.060 log ν + 0.621. According to the Laviron equation [19,51], for an irreversible electrochemical reaction, the relation between E_{pa} and log ν can be expressed as follows:

$$E_{pa} = E^o + \left(\frac{2.303RT}{\alpha nF}\right) log\left(\frac{RTk^o}{\alpha nF}\right) + \left(\frac{2.303RT}{\alpha nF}\right) \log \nu$$

where, E^o is the formal redox potential; k^o is the standard rate constant of the reaction; α is the electron transfer coefficient; n is the electron transfer number involved in the rate-determining step; and R, T and F are standard notation (R = 8.314 J mol^{-1} K^{-1}, T = 298 K, F = 96485C mol^{-1}). According to the linear correlation of E_{pa} versus log ν, as mentioned above, the slope of the line is equal to 2.303RT/αnF, therefore the calculated αn value was 0.985. Generally, α is assumed to be 0.5 for irreversible electrode processes [52]. Thus, the electron transfer number (n) for the oxidation of BPA was assumed to be 2. For the same reaction, n = 2 has also been reported by other authors [4,6,19,26,35,37]. In conclusion, it was verified that the BPA oxidation at the Fe_3O_4 NPs-Si4Pic$^+$Cl$^-$/Au

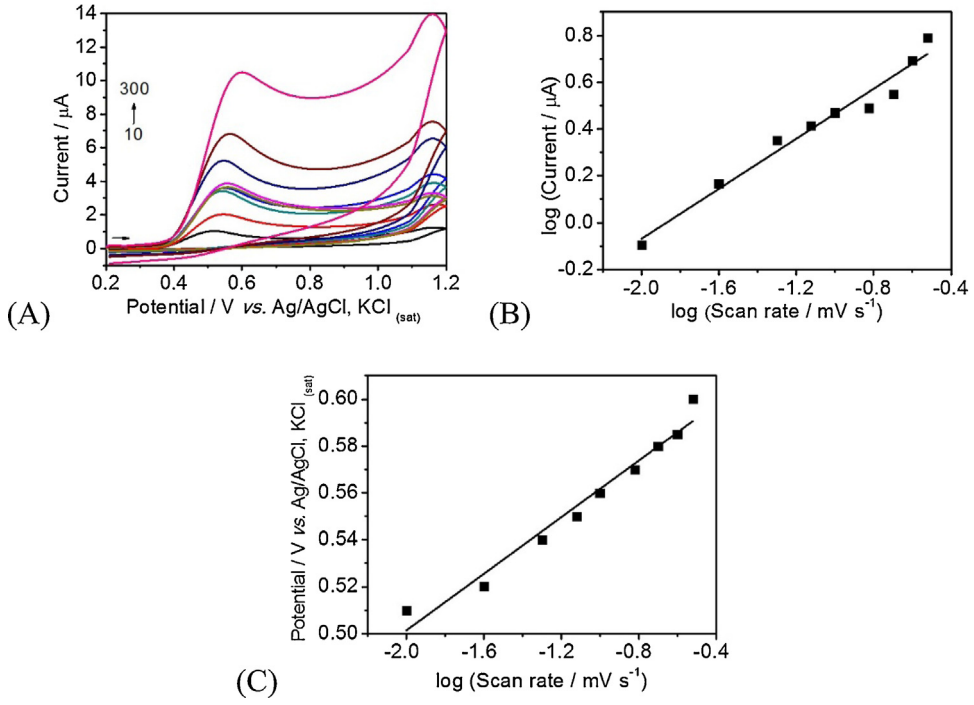

Fig. 6. (A) Cyclic voltammograms of Fe_3O_4 NPs-Si4Pic$^+$Cl$^-$/Au NPs-Si4Pic$^+$Cl$^-$/GCE in 0.1 mol L^{-1} B-R buffer (pH 9.0) containing 10.0 μmol L^{-1} BPA at various scan rates: 10, 25, 50, 75, 100, 150, 200, 250 and 300 mV s^{-1}. The relationship between (B) logarithm of peak current and logarithm of scan rate and (C) anodic peak potential and logarithm of scan rate.

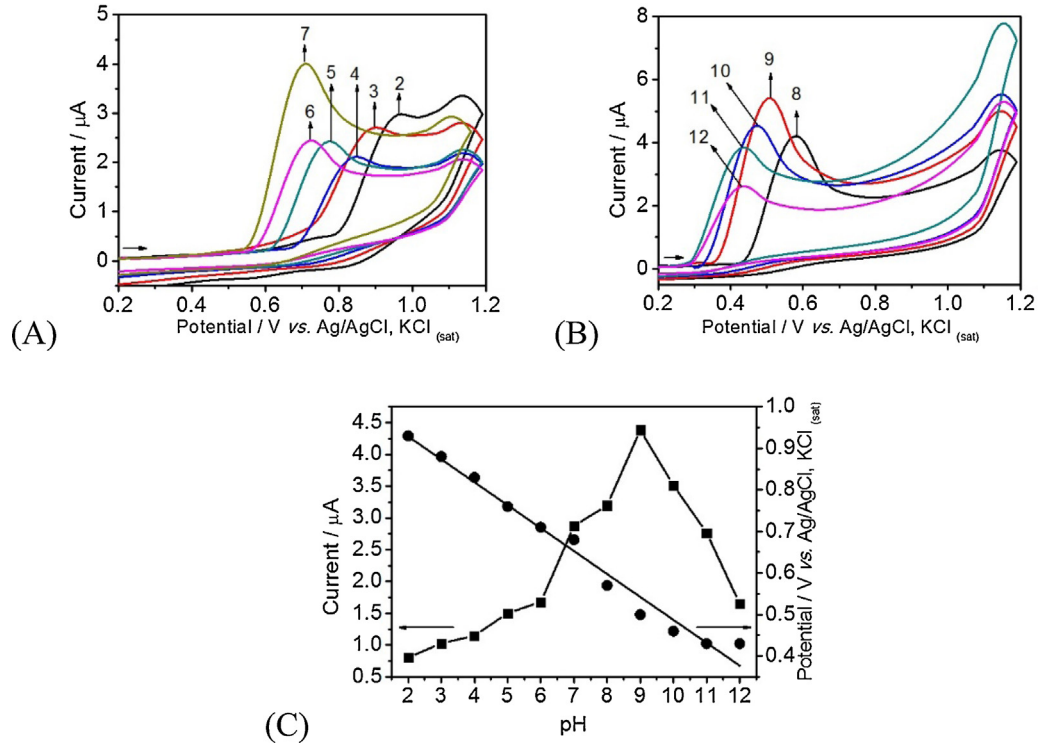

Fig. 7. Cyclic voltammograms for Fe_3O_4 NPs-Si4Pic$^+$Cl$^-$/Au NPs-Si4Pic$^+$Cl$^-$/GCE in 0.1 mol B-R buffer with (A) pH 2.0, 3.0, 4.0, 5.0, 6.0, 7.0 and (B) pH 8.0, 9.0, 10.0, 11.0 and 12.0 containing 10.0 μmol L^{-1} BPA. (C) Effect of pH on the oxidation current and potential, ν = 100 mV s^{-1}.

NPs-Si4Pic$^+$Cl$^-$/GCE is an irreversible diffusion-controlled process involving the participation of two electrons.

3.4. Effect of pH and chemical composition of supporting electrolyte

The pH value of the electrolytic solution is an important factor in relation to the performance of an electrochemical sensor. Therefore, the effect of the solution pH on the electrochemical behavior of BPA was analyzed by cyclic voltammetry using the B-R buffer. The corresponding voltammograms are shown in Fig. 7A and B. The relationship between the oxidation peak current versus pH is best shown in Fig. 7C. As can be seen, the current increased from pH 2.0–9.0 and then decreased. This behavior can be explained by the fact that the solution pH exceeded the pKa value of BPA (*i.e.*, 9.73) [6,37]. Above this value, BPA mainly exists in the ionic form. This result indicates that the non-dissociated form of BPA can be better adsorbed than its dissociated form on the electrode surface, providing a higher oxidation current [34]. Thus, considering the sensitivity in the BPA determination, a pH value of 9.0 was chosen for the subsequent analytical experiments.

Fig. 7. The relationship between the oxidation peak potential and the pH is also shown in Fig. 7C. A linear variation in the E_{pa}, with values moving in the negative potential direction with an increase in the pH, indicated that protons were directly involved in the oxidation of BPA. This variation obeyed the following equation: E_{pa} (V) = −0.0552 pH + 1.039 (R^2 = 0.987). A slope of −55.2 mV pH^{-1} was found, which is close to the theoretical value of −59.2 mV pH^{-1} of the Nernst equation, indicating that equal numbers of electrons and protons were transferred in the oxidation of the BPA on the modified electrode [6,26,34,37].

As described in Section 3.3, the value calculated for the electron transfer number (n) was 2. Thus, the oxidation of BPA on Fe_3O_4 NPs-Si4Pic$^+$Cl$^-$/Au NPs-Si4Pic$^+$Cl$^-$/GCE involved the transfer of two protons and two electrons. Scheme 2 below shows the proposed reaction for BPA oxidation at the Fe_3O_4 NPs-Si4Pic$^+$Cl$^-$/Au NPs-Si4Pic$^+$Cl$^-$/GCE according to the data obtained.

Subsequently, pH values of 8.0 and 9.0 were used to evaluate the influence of different supporting electrolytes on the electrochemical response of BPA. The buffer solutions tested were McIlvaine (pH 8.0), B-R (pH 8.0 and 9.0), H_3BO_3·KCl/NaOH (pH 8.0 and pH 9.0) and NH_3/NH_4Cl (pH 9.0). The highest peak current was obtained in B-R buffer at pH 9.0 (data not shown). Therefore, this buffered solution was chosen for the subsequent analytical experiments.

3.5. Analytical performance

The experimental conditions for the implementation of differential pulse voltammetry (DPV) were optimized with a standard solution of BPA. Applying the optimized conditions, the calibration curve for BPA was constructed in triplicate using the proposed modified electrode Fe_3O_4 NPs-Si4Pic$^+$Cl$^-$/Au NPs-Si4Pic$^+$Cl$^-$/GCE. The differential pulse voltammograms obtained for different concentrations of BPA are shown in Fig. 8A. The calibration curve (Fig. 8B)

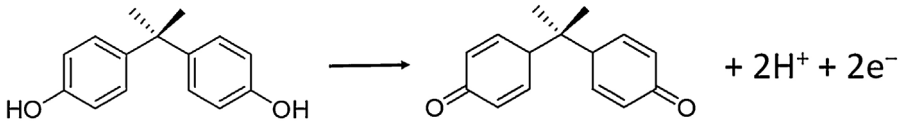

Scheme 2. Proposed reaction for BPA oxidation at the Fe_3O_4 NPs-Si4Pic$^+$Cl$^-$/Au NPs-Si4Pic$^+$Cl$^-$/GCE.

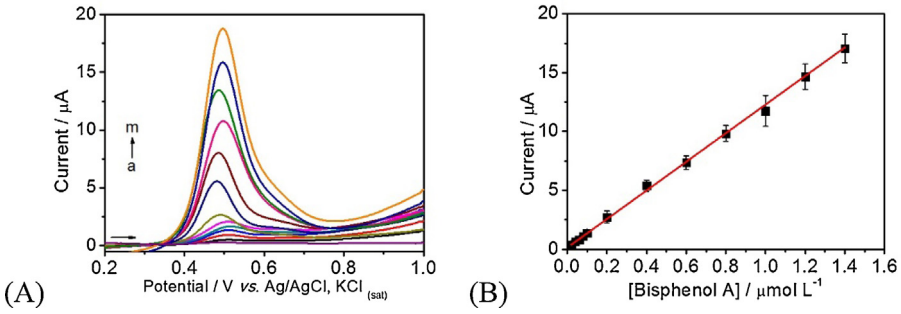

Fig. 8. (A) Differential pulse voltammograms for Fe_3O_4 NPs-Si4Pic$^+$Cl$^-$/Au NPs-Si4Pic$^+$Cl$^-$/GCE in 0.1 mol L^{-1} B-R buffer (pH 9.0) containing BPA (a-m = 0.00, 0.02, 0.04, 0.06, 0.08, 0.10, 0.20, 0.40, 0.60, 0.80, 1.00, 1.20 and 1.40 μmol L^{-1}), ν = 40.0 mV s^{-1}; E_{pulse} = 80.0 mV and t_{pulse} = 8.0 ms. (B) Calibration curve for BPA (n = 3).

Table 1
Analytical parameters of calibration curve for BPA using Fe_3O_4 NPs-Si4Pic$^+$Cl$^-$/Au NPs-Si4Pic$^+$Cl$^-$/GCE.

Analytical parameter	Value
Peak potential (V)	+0.470
Linear range (μmol L^{-1})	0.02 to 1.40
Correlation coefficient – R^2	0.996
Slope (μA L mol^{-1})	12.156
Standard deviation of slope (μA L mol^{-1})	0.139
Intercept (μA)	0.137
Standard deviation of intercept (μA)	0.025
Detection limit (μmol L^{-1})	0.007
Quantification limit (μmol L^{-1})	0.021
Repeatability of i (*intra-day*) (%)[a,b]	4.17
Repeatability of i (*inter-day*) (%)[a,b]	6.79

[a] Relative standard deviation.
[b] n = 5.

was linear from 0.02 to 1.40 μmol L^{-1} BPA, with a correlation coefficient of 0.996. The linear regression equation can be expressed according to the function: i = 12.156[BPA] + 0.137, where i is the resulting peak current in μA, and [BPA] is the concentration of BPA in μmol L^{-1}.

The detection limit (DL) and quantification limit (QL) were calculated according to the equations: DL = 3.3 Sb/B and QL = 10 Sb/B, where Sb is the standard deviation of the linear coefficient and B is the slope of the calibration curve. The DL and QL values obtained were 7.0 nmol L^{-1} and 21.0 nmol L^{-1}, respectively. The analytical parameters extracted from the calibration curve are given in Table 1.

The repeatability of the current measured for the BPA oxidation at the Fe_3O_4 NPs-Si4Pic$^+$Cl$^-$/Au NPs-Si4Pic$^+$Cl$^-$/GCE was estimated in 0.1 mol L^{-1} B-R buffer (pH 9.0) containing 0.6 μmol L^{-1} BPA under optimized conditions. The relative standard deviation (RSD) of successive measurements on the same day (*intra-day* repeatability) was 4.17% (n = 5), indicating good repeatability of the data provided by the modified electrode. The *inter-day* repeatability was evaluated on five consecutive days using the same parameters and a relative standard deviation (RSD) of 6.79% was obtained (n = 5). The Fe_3O_4 NPs-Si4Pic$^+$Cl$^-$ and Au NPs-Si4Pic$^+$Cl$^-$ dispersions were stored at 4 °C in a refrigerator for around three months. During this time, new films were prepared using the same procedure. The relative standard deviation of the analytical response (peak current) for 0.6 μmol L^{-1} BPA using different films was lower than 9.0%, indicating good repeatability for the preparation procedure of the Fe_3O_4 NPs-Si4Pic$^+$Cl$^-$/Au NPs-Si4Pic$^+$Cl$^-$/GCE. Thus, we conclude that the Fe_3O_4 NPs-Si4Pic$^+$Cl$^-$/Au NPs-Si4Pic$^+$Cl$^-$/GCE provides data with high repeatability and, as a consequence, it can be applied for the detection of BPA.

For comparative purposes, Table 2 lists recently published papers reporting the analytical performance of modified electrodes for BPA analysis. It is evident that the LD achieved with the modified electrode proposed herein is one of the lowest values provided by nanomaterial-based modified electrodes. These data verify the ability of the Fe_3O_4 NPs-Si4Pic$^+$Cl$^-$/Au NPs-Si4Pic$^+$Cl$^-$/GCE to detect BPA at nanomolar levels.

3.6. Practical application

Five samples were analyzed in order to determine the BPA content using the two techniques: DPV with the proposed modified electrode and UV–vis spectroscopy. The standard addition method was employed in both techniques and BPA was detected in both cases only in the PC cup samples (see Table 3). The concentration of

Table 2
Performance of different nanomaterial-based modified electrodes for BPA detection.

Modified Electrode	Methods	Linear range (μmol L^{-1})	LD (nmol L^{-1})	Reference
Fe_3O_4 NPs-CS[a]/GCE	DPV	0.05–30.0	8.0	[3]
CMK−3/nano-CILPE[b]	LSV	0.2–150	50.0	[6]
Fe_3O_4 NPs-CB[c]/GCE	DPV	0.0001–50.0	0.031	[19]
Au NPs/SGNF[d]/GCE	LSV	0.08–250.0	35.0	[32]
Au NPs-GR[e]/GCE	DPV	0.0001–100	50.0	[33]
Fe_3O_4 NPs-PANAM[f]/GCE	AMP	0.01–3.07	5.0	[34]
RGO[g]/CNT[h]/Au NPs/SPE[i]	DPV	0.00145–1.49	0.8	[37]
Fe_3O_4 NPs-Si4Pic$^+$Cl$^-$/Au NPs-Si4Pic$^+$Cl$^-$/GCE	DPV	0.02–1.40	7.0	This work

[a] CS: Chitosan.
[b] CMK-3/nano-CILPE: ordered mesoporous carbon modified nano-carbon ionic liquid paste electrode.
[c] CB: carbon black.
[d] SGNF: stacked graphene nanofibers.
[e] Au NPs-GR: gold nanoparticles dotted graphene.
[f] PANAM: poly(amidoamine).
[g] RGO: reduced graphene oxide.
[h] CNT: carbon nanotubes.
[i] SPE: screen printed electrode.

Table 3
Determination of BPA in different samples.

Sample	Determined[a] (μmol L^{-1})		Added (μmol L^{-1})	Found[a] (μmol L^{-1})		Recovery (%)	
	DPV[b]	UV–vis		DPV[b]	UV–vis	DPV[b]	UV–vis
PC cup	0.290	0.275	1.00	1.287	1.272	99–104	97–109
PS plastic cup	---	---	1.00	1.080	0.989	106–112	98–110
PVC food package	---	---	1.00	1.130	1.083	106–120	98–108
PET water bottle	---	---	1.00	1.010	1.021	90–110	101–104
BPA-free plastic	---	---	1.00	1.050	1.011	97–105	93–101

[a] Mean of five measurements under the same conditions.
[b] DPV with Fe_3O_4 NPs-Si4Pic$^+$Cl$^-$/Au NPs-Si4Pic$^+$Cl$^-$/GCE.

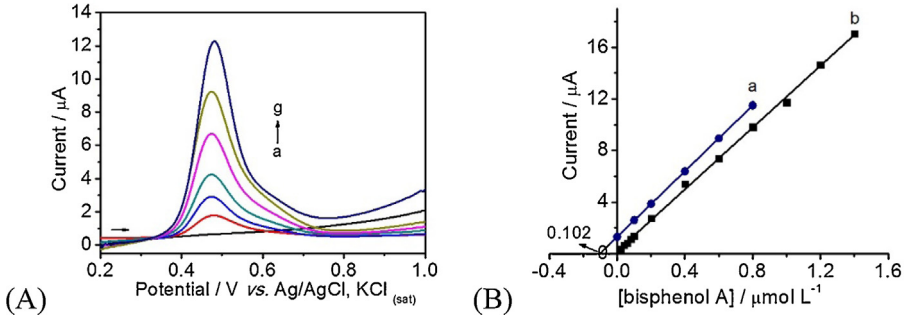

Fig. 9. (A) Differential pulse voltammograms for Fe_3O_4 NPs-Si4Pic$^+$Cl$^-$/Au NPs-Si4Pic$^+$Cl$^-$/GCE modified electrode in 0.1 mol L^{-1} B-R buffer (pH 9.0): (a) blank, (b) PC sample solution, and (c-g) sample with successive additions of 100 μL of 0.1 mmol L^{-1} BPA. (B) The standard addition curve for (a) the PC sample solution and (b) the calibration curve. Experimental conditions: ν = 40.0 mV s^{-1}; E_{pulse} = 80.0 mV and t_{pulse} = 8.0 ms.

BPA determined by the voltammetric method was 0.290 μmol L^{-1} (n = 5, RSD = 6.63%), while according to the spectroscopic method it was 0.275 μmol L^{-1} (n = 5, RSD = 3.72%). To assess the accuracy of the data, recovery experiments were carried out with all samples and the results were between 90% and 120%, which are acceptable values for the concentration level studied.

The results for the determination of BPA in PC cup samples are shown in Fig. 9. Fig. 9A shows the DPVs for the blank (curve a), sample (curve b) and sample with consecutive additions of the BPA standard solution (curves c–g). Fig. 9B shows the resulting standard addition plot (curve a) together with the calibration curve (curve b) for comparison purposes. It can be observed that the slopes of the two curves are very similar. The slope of the calibration curve is 12.156 μA L μmol^{-1} while that of the standard addition curve is 12.730 μA L μmol^{-1}. This verifies that the matrix components of PC cup sample did not interfere in the electrochemical determination of BPA. In addition, the Fe_3O_4 NPs-Si4Pic$^+$Cl$^-$/Au NPs-Si4Pic$^+$Cl$^-$/GCE was able to detect and to discriminate BPA in the presence of the other sample components.

Statistical analysis was applied to compare the sets of data obtained by voltammetric and spectroscopic methods. Two of the most widely used tests for the comparison of data are the *t*-test and *F*-test. The *t*-test method was used to compare the average values for the determination of BPA by the two methods. The calculated t_{value} was 1.75 (confidence level 95%), which was lower than the $t_{theoretical}$ of 2.78. These data indicated that there are no systematic errors in the data provided by the methods used to determine the BPA concentration in PC cup samples. The discrepancy between the data provided by the DPV with the modified electrode Fe_3O_4 NPs-Si4Pic$^+$Cl$^-$/Au NPs-Si4Pic$^+$Cl$^-$/GCE and the UV–vis technique was verified by applying the *F*-test. The F_{value} obtained (3.68) in the quantification of BPA in the PC sample solution was lower than the $F_{theoretical}$ (6.38) at the 95% confidence level, indicating that there is no significant difference in the precision provided by the two techniques. These results corroborate the accuracy and precision of the data obtained with the modified electrode Fe_3O_4 NPs-Si4Pic$^+$Cl$^-$/Au NPs-Si4Pic$^+$Cl$^-$/GCE. The results presented and discussed herein demonstrate that the Fe_3O_4 NPs-Si4Pic$^+$Cl$^-$/Au NPs-Si4Pic$^+$Cl$^-$/GCE provides precise, accurate and reliable data for BPA quantification.

4. Conclusions

A novel and sensitive chemically-modified electrode was successfully employed for the voltammetric determination of BPA, based on Fe_3O_4 NPs and Au NPs both stabilized in a polymer solution of Si4Pic$^+$Cl$^-$. Due to the combination of the electrocatalytic and high conductivity properties of the nanoparticles used, the proposed modified electrode improved the oxidation of BPA, increasing its oxidation peak current and lowering its oxidation potential. The calibration curve was constructed in a concentration range of 20 nm to 1400 nmol L^{-1}. The LD was 7.0 nmol L^{-1}, which is one of the lowest provided by modified electrodes. The proposed modified electrode Fe_3O_4 NPs-Si4Pic$^+$Cl$^-$/Au NPs-Si4Pic$^+$Cl$^-$/GCE was successfully applied in the determination of BPA in commercial plastic samples showing excellent accuracy, as observed from recovery experiments and comparison with data obtained by UV–vis spectroscopy. Moreover, the results obtained using the modified electrode also showed high precision, which was evaluated by statistical processing of the data. Hence, the proposed Fe_3O_4 NPs-Si4Pic$^+$Cl$^-$/Au NPs-Si4Pic$^+$Cl$^-$/GCE associated with DPV is an effective device to determine BPA and potentially other endocrine disruptors with similar chemical structure.

Acknowledgements

The authors are grateful to the Brazilian government agencies CAPES (Coordenação de Aperfeiçoamento de Pessoal de Nível Superior) for the scholarships awarded to ERS and CAL and CNPq (Conselho Nacional de Desenvolvimento Científico e Tecnológico) for the financial support and scholarship awarded to JVP and AS. This research was also supported by the Central Laboratory of Electron Microscopy of Federal University of Santa Catarina

(Florianópolis/SC, Brazil) and FAPESC (Fundação de Amparo à Pesquisa e Inovação do Estado de Santa Catarina).

References

[1] G.F. Pereira, L.S. Andrade, R.C. Rocha-Filho, N. Bocchi, S.R. Biaggio, Electrochemical determination of bisphenol A using a boron-doped diamond electrode, Electrochim. Acta 82 (2012) 3–8.
[2] K.V. Ragavan, N.K. Rastogi, M.S. Thakur, Sensors and biosensors for analysis of bisphenol A, TrAC Trends Anal. Chem. 52 (2013) 248–260.
[3] C. Yu, L. Gou, X. Zhou, N. Bao, H. Gu, Chitosan-Fe_3O_4 nanocomposite based electrochemical sensors for the determination of bisphenol A, Electrochim. Acta 56 (2011) 9056–9063.
[4] Y. Gao, Y. Cao, D. Yang, X. Luo, Y. Tang, H. Li, Sensitivity and selectivity determination of bisphenol A using SWCNT-CD conjugate modified glassy carbon electrode, J. Hazard. Mater. 199–200 (199) (2012) 111–118.
[5] X. Zhang, L. Wu, J. Zhou, X. Zhang, J. Chen, A new ratiometric electrochemical sensor for sensitive detection of bisphenol A based on poly-β-cyclodextrin/electroreduced graphene modified glassy carbon electrode, J. Electroanal. Chem. 742 (2015) 97–103.
[6] Y. Li, X. Zhai, X. Liu, L. Wang, H. Liu, H. Wang, Electrochemical determination of bisphenol A at ordered mesoporous carbon modified nano-carbon ionic liquid paste electrode, Talanta 148 (2016) 362–369.
[7] X. Xin, S. Sun, H. Li, M. Wang, R. Jia, Electrochemical bisphenol A sensor based on core–shell multiwalled carbon nanotubes/graphene oxide nanoribbons, Sens. Actuators B 209 (2015) 275–280.
[8] Y. Watabe, T. Kondo, M. Morita, N. Tanaka, J. Haginaka, K. Hosoya, Determination of bisphenol A in environmental water at ultra-low level by high-performance liquid chromatography with an effective on-line pretreatment device, J. Chromatogr. A 1032 (2004) 45–49.
[9] A. Ballesteros-Gómez, S. Rubio, D. Pérez-Bendito, Analytical methods for the determination of bisphenol A in food, J. Chromatogr. A 1216 (2009) 449–469.
[10] A. Halle, C. Claparols, J.C. Garrigues, S. Franceschi-Messant, E. Perez, Development of an extraction method based on new porous organogel materials coupled with liquid chromatography–mass spectrometry for the rapid quantification of bisphenol A in urine, J. Chromatogr. A 1414 (2015) 1–9.
[11] S.C. Cunha, A. Pena, J.O. Fernandes, Dispersive liquid–liquid microextraction followed by microwave-assisted silylation and gas chromatography-mass spectrometry analysis for simultaneous trace quantification of bisphenol A and 13 ultraviolet filters in wastewaters, J. Chromatogr. A 1414 (2015) 10–21.
[12] L. Zhu, Y. Cao, G. Cao, Electrochemical sensor based on magnetic molecularly imprinted nanoparticles at surfactant modified magnetic electrode for determination of bisphenol A, Biosens. Bioelectron. 54 (2014) 258–261.
[13] Y. Li, J. Xu, L. Wang, Y. Huang, J. Guo, X. Cao, F. Shen, Y. Luo, C. Sun, Chemical aptamer-based fluorescent detection of bisphenol A using nonconjugated gold nanoparticles and CdTe quantum dots, Sens. Actuators B 222 (2016) 815–822.
[14] H. Huang, Y. Li, J. Liu, J. Tong, X. Su, Detection of bisphenol A in food packaging based on fluorescent conjugated polymer $PPESO_3$ and enzyme system, Food Chem. 185 (2015) 233–238.
[15] W. Miao, B. Wei, R. Yang, C. Wu, D. Lou, W. Jiang, Z. Zhou, Highly specific and sensitive detection of bisphenol A in water samples using an enzyme-linked immunosorbent assay employing, New J. Chem. 38 (2014) 15–17.
[16] C. Lu, J. Li, Y. Yang, J. Lin, Determination of bisphenol A based on chemiluminescence from gold(III)–peroxymonocarbonate, Talanta 82 (2010) 1576–1580.
[17] M. Amjadi, J.L. Manzoori, T. Hallaj, A novel chemiluminescence method for determination of bisphenol A based on the carbon dot-enhanced HCO_3^-–H_2O_2 system, J. Lumin. 158 (2015) 160–164.
[18] B. Nikahd, M.A. Khalilzadeh, Liquid phase determination of bisphenol A in food samples using novel nanostructure ionic liquid modified sensor, J. Mol. Liq. 215 (2016) 253–257.
[19] C. Hou, W. Tang, C. Zhang, Y. Wang, N. Zhu, A novel and sensitive electrochemical sensor for bisphenol A determination based on carbon black supporting ferroferric oxide nanoparticles, Electrochim. Acta 144 (2014) 324–331.
[20] J. Wang, Y. Su, B. Wu, S. Cheng, Reusable electrochemical sensor for bisphenol A based on ionic liquid functionalized conducting polymer platform, Talanta 147 (2016) 103–110.
[21] R.S.J. Alkasir, M. Ganesana, Y. Won, L. Stanciu, S. Andreescu, Enzyme functionalized nanoparticles for electrochemical biosensors: a comparative study with applications for the detection of bisphenol A, Biosens. Bioelectron. 26 (2010) 43–49.
[22] J. Kochana, K. Wapiennik, J. Kozak, P. Knihnicki, A. Pollap, M. Woźniakiewicz, J. Nowak, P. Kościelniak, Tyrosinase-based biosensor for determination of bisphenol A in a flow-batch system, Talanta 144 (2015) 163–170.
[23] L. Kou, R. Liang, X. Wang, Y. Chen, W. Qin, Potentiometric sensor for determination of neutral bisphenol A using a molecularly imprinted polymer as a receptor, Anal. Bioanal. Chem. 405 (2013) 4931–4936.
[24] S. Dadkhar, E. Ziaei, A. Mehdinia, T.B. Kayyal, A. Jabbari, A glassy carbon electrode modified with amino-functionalized graphene oxide and molecularly imprinted polymer for electrochemical sensing of bisphenol A, Microchim. Acta 183 (2016) 1933–1941.
[25] L.A. Goulart, F.C. Moraes, L.H. Mascaro, Influence of the carbon nanotubes on the development of electrochemical sensors for bisphenol A, Mat. Sci. Eng. C-Mater. 58 (2016) 768–773.
[26] Y. Li, Y. Gao, Y. Cao, H. Li, Electrochemical sensor for bisphenol A determination based on MWCNT/melamine complex modified GCE, Sens. Actuators B 171–172 (2012) 726–733.
[27] J. Yi, S. Tang, Z. Wang, Y. Yin, S. Yang, B. Zhang, S. Shu, T. Liu, L. Xu, Electrochemical determination of bisphenol A based on PHD/MWCNTs modified glassy carbon electrode, Inter. J. Environ. Anal. Chem. 95 (2015) 158–174.
[28] J. Wan, Y. Si, C. Li, K. Zhang, Bisphenol A electrochemical sensor based on multi-walled carbon nanotubes/polythiophene/Pt nanocomposites modified electrode, Anal. Methods 8 (2016) 3333–3338.
[29] H. Fan, Y. Li, D. Wu, H. Ma, K. Mao, D. Fan, B. Du, H. Li, Q. Wei, Electrochemical bisphenol A sensor based on N-doped graphene sheets, Anal. Chim. Acta 711 (2012) 24–28.
[30] E.B. Bahadir, M.K. Sezgintürk, Applications of graphene in electrochemical sensing and biosensing, TrAC Trends Anal. Chem. 76 (2016) 1–14.
[31] F. Tan, L. Cong, X. Li, Q. Zhao, H. Zhao, X. Quan, J. Chen, An electrochemical sensor based on molecularly imprinted polypyrrole/graphene quantum dots composite for detection of bisphenol A in water samples, Sens. Actuators B 233 (2016) 599–606.
[32] X. Niu, W. Yang, G. Wang, J. Ren, H. Guo, J. Gao, A novel electrochemical sensor of bisphenol A based on stacked graphene nanofibers/gold nanoparticles composite modified glassy carbon electrode, Electrochim. Acta 98 (2013) 167–175.
[33] L. Zhou, J. Wang, D. Li, Y. Li, An electrochemical aptasensor based on gold nanoparticles dotted graphene modified glassy carbon electrode for label-free detection of bisphenol A in milk samples, Food Chem. 162 (2014) 34–40.
[34] H. Yin, L. Cui, Q. Chen, W. Shi, S. Ai, L. Zhu, L. Lu, Amperometric determination of bisphenol A in milk using PAMAM–Fe_3O_4 modified glassy carbon electrode, Food Chem. 125 (2011) 1097–1103.
[35] Y. Zhang, Y. Cheng, Y. Zhou, B. Li, W. Gu, X. Shi, Y. Xian, Electrochemical sensor for bisphenol A based on magnetic nanoparticles decorated reduced graphene oxide, Talanta 107 (2013) 211–218.
[36] K. Saha, S.S. Agasti, C. Kim, X. Li, V.M. Rotello, Gold nanoparticles in chemical and biological sensing, Chem. Rev. 112 (2012) 2739–2779.
[37] Y. Wang, D. Cokeliler, S. Gunasekaran, Reduced graphene oxide/carbon nanotube/gold nanoparticles nanocomposite functionalized screen-printed electrode for sensitive electrochemical detection of endocrine disruptor bisphenol A, Electroanalysis 27 (2015) 2527–2536.
[38] S. Erogul, S.Z. Bas, M. Ozmen, S. Yildiz, A new electrochemical sensor based on Fe_3O_4 functionalized graphene oxide-gold nanoparticle composite film for simultaneous determination of catechol and hydroquinone, Electrochim. Acta 186 (2015) 302–313.
[39] A. Afkhami, F. Soltani-Felehgari, T. Madrakian, Gold nanoparticles modified carbon paste electrode as an efficient electrochemical sensor for rapid and sensitive determination of cefixime in urine and pharmaceutical samples, Electrochim. Acta 103 (2013) 125–133.
[40] S. Afonso, B. Pérez-López, R.C. Faria, L.H.C. Mattoso, M. Hernández-Herrero, A.X. Roig-Sagués, M.M. Costa, A. Merkoçi, Electrochemical detection of *Salmonella* using gold nanoparticles, Biosens. Bioelectron. 40 (2013) 121–126.
[41] G. Chen, H. Tong, T. Gao, Y. Chen, G. Li, Direct application of gold nanoparticles to one-pot electrochemical biosensors, Anal. Chim. Acta 849 (2014) 1–6.
[42] V. Vinoth, J.J. Wu, A.M. Asiri, S. Anandan, Simultaneous detection of dopamine and ascorbic acid using silicate network interlinked gold nanoparticles and multi-walled carbon nanotubes, Sens. Actuators B 210 (2015) 731–741.
[43] P.S. Silva, B.C. Gasparini, H.A. Magosso, A. Spinelli, Gold nanoparticles hosted in a water-soluble silsesquioxane polymer applied as a catalytic material onto an electrochemical sensor for detection of nitrophenol isomers, J. Hazard. Mater. 273 (2014) 70–77.
[44] J. Xu, F. Zhang, J. Sun, J. Sheng, F. Wang, M. Sun, Bio and nanomaterials based on Fe_3O_4, Molecules 19 (2014) 21506–21528.
[45] A.C. Schneid, M.B. Pereira, F. Horowitz, R.S. Mauler, C.R. Matte, M.P. Klein, E.W. Menezes, E.V. Benvenutti, Silver nanoparticle thin films deposited on glass surface using an ionic silsesquioxane as stabilizer and as crosslinking agent, J. Braz. Chem. Soc. 26 (2015) 1004–1012.
[46] M. Deon, E.M. Caldas, D.S. da Rosa, E.W. de Menezes, S.L.P. Dias, M.P. Pereira, T.M.H. Costa, L.T. Arenas, E.V. Benvenutti, Mesoporous silica xerogel modified with bridged ionic silsesquioxane used to immobilize copper tetrasulfonated phthalocyanine applied to electrochemical determination of dopamine, J. Solid State Electrochem. 19 (2015) 2095–2105.
[47] S. Link, M.A. El-Sayed, Size and temperature dependence of the plasmon absorption of colloidal gold nanoparticles, J. Phys. Chem. B 103 (1999) 4212–4217.
[48] S. Zeng, K. Yong, I. Roy, X. Dinh, X. Yu, F. Luan, A review on functionalized gold nanoparticles for biosensing applications, Plasmonics 6 (2011) 491–506.
[49] Z. Zheng, Y. Du, Z. Wang, Q. Feng, C. Wang, Pt/graphene–CNTs nanocomposite based electrochemical sensors for the determination of endocrine disruptor bisphenol A in thermal printing papers, Analyst 138 (2013) 693–701.
[50] K.D. Gosser, Cyclic Voltammetry: Simulation and Analysis of Reaction Mechanisms, VCH New York, 1993.
[51] E. Laviron, Adsorption, autoinhibition and autocatalysis in polarography and in linear potential sweep voltammetry, J. Electroanal. Chem. 52 (1974) 355–393.

[52] A.J. Bard, L.R. Faulkner, Electrochemical Methods: Fundamentals and Applications, second ed., Wiley, New York, 2001.

Biographies

Edson R. Santana is a Master's degree student at the Federal University of Santa Catarina, Florianópolis, Brazil. His research work is concentrated on the use of modified electrodes for the electroanalytical determination of compounds of biological and environmental interest.

Camila A. de Lima received her Doctorate in Analytical Chemistry in 2016 from Federal University of Santa Catarina, Florianópolis, Brazil. Her research interest is concentrated on the development of electrodes for the electroanalytical determination of organic and inorganic compounds.

Jamille V. Piovesan is a PhD student at the Federal University of Santa Catarina, Florianópolis, Brazil. Her research work is concentrated on the development of new modified electrodes for the electroanalytical determination of organic compounds of biological and environmental interest.

Almir Spinelli received his Doctorate in Applied Electrochemistry from the University of Poitiers, France, in 1992. Currently, he is a full-time professor and researcher at Department of Chemistry of the Federal University of Santa Catarina, Florianópolis, Brazil. His research focuses on electrochemical processes, as well as electroanalytical determinations and corrosion studies.